Heart Vessels (2016) 31:773–782
DOI 10.1007/s00380-015-0672-2

ORIGINAL ARTICLE

Left atrial electrophysiologic feature specific for the genesis of complex fractionated atrial electrogram during atrial fibrillation

Tadashi Hoshiyama[1] · Hiroshige Yamabe[1] · Junjiroh Koyama[1] · Hisanori Kanazawa[1] · Hisao Ogawa[1]

Received: 26 September 2014 / Accepted: 1 April 2015 / Published online: 9 April 2015
© Springer Japan 2015

Abstract Complex fractionated atrial electrogram (CFAE) has been suggested to contribute to the maintenance of atrial fibrillation (AF). However, electrophysiologic characteristics of the left atrial myocardium responsible for genesis of CFAE have not been clarified. Non-contact mapping of the left atrium was performed at 37 AF onset episodes in 24 AF patients. Electrogram amplitude, width, and conduction velocity were measured during sinus rhythm, premature atrial contraction (PAC) with long- (L-PAC), short- (S-PAC) and very short-coupling intervals (VS-PAC). These parameters were compared between CFAE and non-CFAE regions. Unipolar electrogram amplitude was higher in CFAE than non-CFAE during sinus rhythm, L-, S- and VS-PAC (1.82 ± 0.73 vs. 1.13 ± 0.38, $p < 0.001$; 1.44 ± 0.54 vs. 0.92 ± 0.35, $p < 0.001$; 1.09 ± 0.40 vs. 0.70 ± 0.27, $p < 0.001$; 0.76 ± 0.30 vs. 0.53 ± 0.25 mV, $p < 0.001$). Laplacian bipolar electrogram amplitude was also higher in CFAE than non-CFAE during sinus rhythm, L-, S- and VS-PAC. Unipolar electrogram width was similar in CFAE and non-CFAE. Laplacian bipolar electrogram width was wider in CFAE than non-CFAE during L-, S- and VS-PAC (85.5 ± 6.8 vs. 79.6 ± 4.5, $p < 0.001$; 96.1 ± 9.7 vs. 84.5 ± 5.9, $p < 0.001$; 122.4 ± 16.0 vs. 99.6 ± 9.6 ms, $p < 0.001$), but not during sinus rhythm. The conduction velocity was slower in CFAE during sinus rhythm, L-, S- and VS-PAC than non-CFAE (1.7 ± 0.3 vs. 2.4 ± 0.4, $p < 0.001$; 1.4 ± 0.3 vs. 2.0 ± 0.5, $p < 0.001$; 1.2 ± 0.3 vs. 1.7 ± 0.5, $p < 0.001$; and 0.9 ± 0.3 vs. 1.4 ± 0.4 m/s, $p < 0.001$). CFAE was generated in the high amplitude atrial myocardium with slow and non-uniform conduction properties which were pronounced associated with premature activation, suggesting that heterogeneous conduction produced in high amplitude region contributes to the genesis of CFAE.

Keywords Atrial fibrillation · Complex fractionated atrial electrogram · Non-contact mapping · Electrophysiology

Introduction

Catheter ablation of complex fractionated atrial electrogram (CFAE), combined with pulmonary vein (PV) isolation, is an effective treatment for atrial fibrillation (AF) [1, 2]. Konings et al. [3] indicated that CFAEs are found mostly in the slow conduction areas or pivot points where the activation wavefront turns around the end of arcs of functional blocks. Based on their findings, Nademanee et al. [4] suggested that CFAEs are the ideal target sites for catheter ablation of AF. We have recently shown that the CFAE region plays an important role in the perpetuation of AF [5]. Our results showed that the slow conduction and pivoting activation following the wave break and wave fusion observed in the CFAE sustained AF [5]. In another study, we also indicated that unidirectional conduction block, which is critical for the initiation of random reentrant wave propagation, was produced in the CFAE region at the onset of AF [6]. However, the electrophysiological features of the left atrial myocardium, which is responsible for the genesis of CFAE, have not been clarified.

This study was presented in part at the 84th Scientific Sessions of the American Heart Association, Orlando, FL, November 12–17, 2011.

✉ Hiroshige Yamabe
yyamabe@kumamoto-u.ac.jp

[1] Department of Cardiovascular Medicine, Graduate School of Medical Sciences, Kumamoto University, 1-1-1 Honjo, Kumamoto 860-8556, Japan

In the present study, we examined the dynamic changes in various electrophysiological parameters of the left atrial myocardium associated with the change in prematurity of the left atrial contractions. Thus, we elucidated the atrial amplitude, electrogram width and conduction velocity, both during sinus rhythm and premature contractions at different coupling intervals that had been observed at AF onset. Furthermore, we compared these electrophysiological parameters between the CFAE and non-CFAE regions to define the specific nature of the left atrial myocardium in the genesis of CFAE.

Methods

Patient population

Study population comprised 156 consecutive patients who had undergone their first catheter ablation for AF at the Kumamoto University hospital between October 2006 and February 2012. In those 156 patients, endocardial mapping of the left atrium (LA) was performed using a non-contact mapping system in 92 patients. Among these 92 patients, 24 patients in whom the spontaneous AF onset was documented during electrophysiological studies (22 men and 2 women; mean age 58 years, range 34–79 years) were included in this study. The remaining 68 patients in whom the spontaneous AF was not observed, but was induced by atrial pacing were excluded. There were 22 patients with paroxysmal AF and 2 patients with persistent AF. The mean duration of AF was 4.1 ± 2.2 years. The left ventricular ejection fraction and left atrial dimension, measured on the echocardiography, were 64.1 ± 5.8 % and 37.1 ± 4.8 mm, respectively. The study protocol was approved by the Human Research Committee of Kumamoto University Hospital and a written informed consent was obtained from each patient.

Electrophysiological study and image acquisition

All antiarrhythmic drugs were discontinued for at least five half-lives before the electrophysiological study and ablation procedure. A 6-Fr 20-pole and a 6-Fr quadripolar electrode catheters (St. Jude Medical, St. Paul, MN, USA) were inserted percutaneously and their tips positioned in the coronary sinus and right ventricular apex, respectively. An atrial transseptal puncture was performed under fluoroscopic guidance, and two 8-Fr long sheaths (St. Jude Medical) were advanced into the LA. Intravenous heparin was administered after transseptal puncture to maintain an activated clotting time of between 300 and 350 s. After left atriography, one 8-Fr long sheath was exchanged for a 10-Fr sheath. A 9-Fr multi-electrode array catheter was introduced into the LA via the 10-Fr sheath, deployed on a 0.032-inch guidewire with its distal tip fixed in the left superior PV. A 7-Fr large-tip (8 mm in length) deflectable quadripolar electrode catheter (Japan Lifeline, Tokyo, Japan) was used for mapping and ablation. Bipolar electrograms were filtered between 50 and 600 Hz and recorded along with the surface electrocardiogram using polygraph (EP-workmate; EP Med. Systems, Inc., Mt Arlington, NJ, USA). Pacing was performed using a cardiac stimulator (SEC-4103; Nihon Kohden, Tokyo, Japan).

Non-contact mapping system

Endocardial mapping of the LA was performed using a non-contact mapping system (EnSite 3000; St. Jude Medical, MN). The details of the EnSite 3000 System have been described previously [5].

Study protocol

Localization of CFAE region

The location of the CFAE region was identified by non-contact virtual unipolar and virtual Laplacian bipolar electrograms observed during AF. The CFAE was defined using the following criteria [4]: (1) atrial electrograms with fractionated electrograms composed of two deflections or more, and/or perturbation of baseline with continuous deflection of a prolonged activation complex over a 10-s recording period; and, (2) atrial electrograms with a very short cycle length (<120 ms) averaged over a 10-s recording period. The CFAE area was calculated by the sum of all CFAE regions in the LA. The location of the CFAE region was agreed upon by two independent observers.

Electrophysiological parameters analyzed during sinus rhythm and premature contraction

To elucidate the change in electrophysiological parameters with various coupling intervals of atrial contraction, the activation sequence at the spontaneous onset of sustained AF was analyzed utilizing the non-contact mapping system. The electrogram amplitude and electrogram width of the unipolar and Laplacian bipolar electrograms, in addition to the conduction velocity, were measured during sinus rhythm and premature atrial contraction (PAC) with various coupling intervals. The electrogram amplitude and width represented the average of 10 points that were arbitrarily chosen both in CFAE and non-CFAE region in each episode. These 10 points throughout the CFAE and non-CFAE region, which were equally distributed, were collected to ensure complete coverage of each area. The conduction velocity represented the difference in activation

time over a measurable distance, which was traced on the wavefront path. PAC was classified into three categories: (1) PAC with the longest coupling interval that did not initiate the AF at the onset of AF was defined as long PAC (L-PAC). (2) PAC with the shortest coupling interval that was observed just before the AF onset and initiated AF was defined as very short PAC (VS-PAC). PAC with the coupling interval between the L-PAC and VS-PAC that did not initiate AF was defined as short PAC (S-PAC). AF onset associated with the initiation of continuous wave propagation was verified by the non-contact mapping. The electrogram amplitude, electrogram width and conduction velocity during sinus rhythm, L-PAC, S-PAC and VS-PAC were compared between the CFAE and non-CFAE regions. All of the electrophysiological parameters were measured manually by two independent observers in the absence of prior LA ablation.

Statistical analysis

Values are expressed as mean ± standard deviation. One way analysis of variance (ANOVA) with Fisher's Least Significant Difference test was used for multiple comparisons of the data. A paired *t* test was used for comparisons between the parameters of CFAE and non-CFAE regions. All statistical analyses were performed using SPSS. A p value <0.05 denoted the presence of statistically significant difference.

Results

A total of 37 episodes of spontaneous AF onset were encountered in the present study, which were initiated by focal discharges. The electrophysiological parameters of these 37 episodes were analyzed. AF onset associated with subsequent continuous random wave propagation was verified in all patients.

Distribution of CFAE

CFAEs were recorded in all patients during AF. The CFAE area was 18.6 ± 11.1 cm^2 (28 ± 17 % of the LA). The distribution of CFAE was as follows: LA roof (24 patients, 100 %); LA septum (17 patients, 70 %); LA anterior (11 patients, 46 %); LA appendage (7 patients, 29 %); LA posterior (3 patients, 13 %); left superior PV (15 patients, 62 %); right superior PV (15 patients, 62 %); left inferior PV (2 patients, 8 %); and right inferior PV (1 patient, 4 %). Therefore, the LA roof, LA septum and PV were the preferable site of CFAE region. The coupling interval of VS-PAC (169.1 ± 28.9 ms) was shorter than that of L-PAC (310.2 ± 84.7 ms, $p < 0.001$) and S-PAC (209.8 ± 44.2 ms, $p < 0.001$). Also, S-PAC was shorter than that of L-PAC ($p < 0.001$).

Comparison of amplitudes of unipolar and Laplacian bipolar electrograms between CFAE and non-CFAE

The amplitude of unipolar electrogram significantly decreased following shortening of the coupling interval in both CFAE (Fig. 1a) and non-CFAE regions (Fig. 1b). Furthermore, the amplitude of unipolar electrogram in the CFAE region was significantly higher than that in the non-CFAE region during sinus rhythm, L-, S- and VS-PAC (1.82 ± 0.73 vs. 1.13 ± 0.38, $p < 0.001$; 1.44 ± 0.54 vs. 0.92 ± 0.35, $p < 0.001$; 1.09 ± 0.40 vs. 0.70 ± 0.27, $p < 0.001$; 0.76 ± 0.30 vs. 0.53 ± 0.25 mV, $p < 0.001$, respectively) (Fig. 1c).

The amplitudes of Laplacian bipolar electrograms significantly decreased following shortening of the coupling interval in both CFAE (Fig. 1d) and non-CFAE regions (Fig. 1e). Furthermore, the amplitude of the Laplacian bipolar electrogram was significantly higher in the CFAE region than that in the non-CFAE region during sinus rhythm, L-, S- and VS-PAC (1.77 ± 0.86 vs. 0.22 ± 0.11, $p < 0.001$; 1.17 ± 0.64 vs. 0.16 ± 0.10, $p < 0.001$; 0.76 ± 0.46 vs. 0.10 ± 0.07, $p < 0.001$; 0.45 ± 0.21 vs. 0.06 ± 0.03 mV, $p < 0.001$, respectively) (Fig. 1f).

Comparison of electrogram width between CFAE and non-CFAE regions

Prolongation of the unipolar electrogram width was noted following shortening of the coupling interval of PAC in both CFAE (Fig. 2a) and non-CFAE regions (Fig. 2b). There was no significant difference in unipolar electrogram width between the CFAE and non-CFAE regions during sinus rhythm, L-, S- and VS-PAC (66.7 ± 6.1 vs. 67.2 ± 5.8, $p = 0.073$; 75.6 ± 7.2 vs. 76.0 ± 7.2, $p = 0.137$; 91.0 ± 10.2 vs. 90.4 ± 10.1, $p = 0.092$; 117.3 ± 21.7 vs. 116.8 ± 21.7 ms, $p = 0.069$, respectively) (Fig. 2c).

Prolongation of the Laplacian bipolar electrogram width was also noted following shortening of coupling interval of PAC in both CFAE (Fig. 2d) and non-CFAE regions (Fig. 2e).The Laplacian bipolar electrogram width was not different in the CFAE and non-CFAE regions during sinus rhythm (74.5 ± 4.8 vs. 74.2 ± 4.9 ms, $p = 0.526$). However, the Laplacian bipolar electrogram width in the CFAE region was significantly wider in the CFAE region than the non-CFAE region during L-, S- and VS-PAC (85.5 ± 6.8 vs. 79.6 ± 4.5, $p < 0.001$; 96.1 ± 9.7 vs. 84.5 ± 5.9, $p < 0.001$; 122.4 ± 16.0 vs. 99.6 ± 9.6 ms, $p < 0.001$, respectively) (Fig. 2f).

Figure 3 shows the percentage of increment in Laplacian bipolar electrogram width during L-, S- and VS-PAC

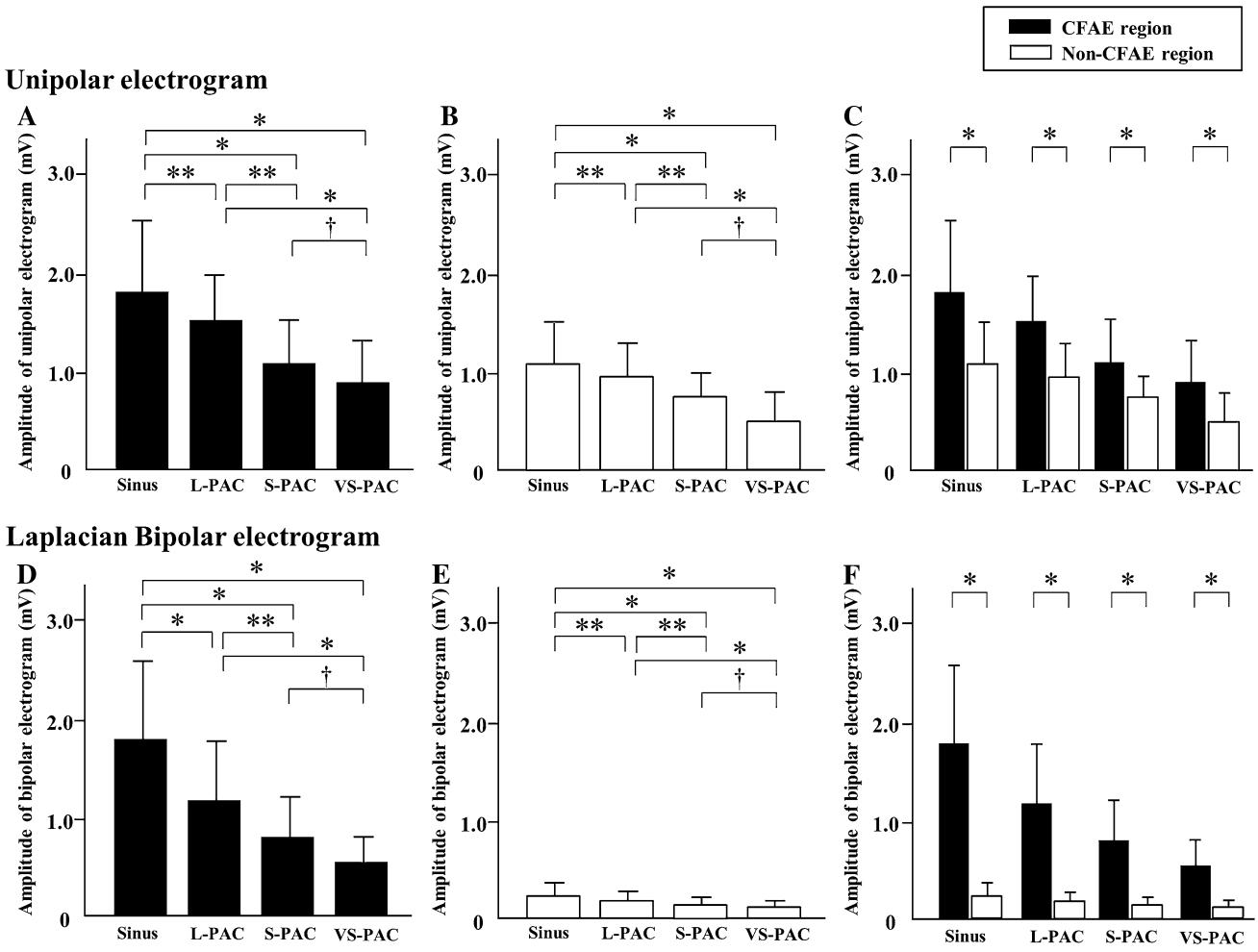

Fig. 1 Amplitude of the unipolar electrograms during sinus rhythm, L-, S- and VS-PAC in the CFAE region (**a**) and in the non-CFAE region (**b**) are shown. **c** Differences in the unipolar electrograms during sinus rhythm, L-PAC, S-PAC and VS-PAC between the CFAE and the non-CFAE regions. Amplitude of the Laplacian bipolar electrograms during sinus rhythm, L-, S- and VS-PAC in CFAE region (**d**) and those in non-CFAE region (**e**) are shown. **f** Differences in the Laplacian bipolar electrograms during sinus rhythm, L-PAC, S-PAC and VS-PAC between the CFAE and the non-CFAE regions $^{*}p < 0.001$, $^{**}p < 0.01$, $^{\dagger}p < 0.05$

relative to baseline sinus rhythm in CFAE and non-CFAE regions. The increment was significantly greater in CFAE than in non-CFAE region during L-, S- and VS-PAC (15.7 ± 7.5 vs. 9.0 ± 7.8, $p < 0.001$; 30.4 ± 13.0 vs. 15.2 ± 8.8, $p < 0.001$; 62.7 ± 21.1 vs. 33.6 ± 12.8 %, $p < 0.001$, respectively). The increment was especially evident during VS-PAC (Fig. 3).

Figure 4 shows two representative Laplacian bipolar electrograms recorded in CFAE (site A) and non-CFAE (site B) sites at AF onset. AF was initiated following four PACs derived from the right superior PV. The first PAC with the longest coupling interval (230 ms) was assigned as L-PAC and the 4th PAC with the shortest coupling interval (140 ms) was assigned as VS-PAC. The 2nd PAC with the coupling interval of 165 ms, which is shorter than the coupling interval of L-PAC (230 ms) and longer than that of VS-PAC (140 ms), was assigned as S-PAC. The amplitude of the Laplacian bipolar electrogram decreased following shortening of the coupling interval of PAC in both the CFAE and non-CFAE sites. The electrogram amplitudes during sinus rhythm, L-, S- and VS-PAC in CFAE site (2.87, 1.74, 1.52 and 0.89 mV) were all higher than those in the non-CFAE site (0.93, 0.61, 0.41 and 0.34 mV). Prolongation of the Laplacian bipolar electrogram width was evident after shortening of the coupling intervals in both the CFAE and non-CFAE sites. The electrogram width in CFAE site was not different from that in non-CFAE site during sinus rhythm (71 vs. 71 ms). However, it was wider during L-, S- and VS-PAC in the CFAE site (82, 98 and 119 ms) than in the non-CFAE site (78, 86 and 97 ms).

Figure 5 shows the unipolar electrograms in CFAE (site A) and non-CFAE (site B) sites at AF onset in the same patient shown in Fig. 4. The amplitude of the unipolar electrogram

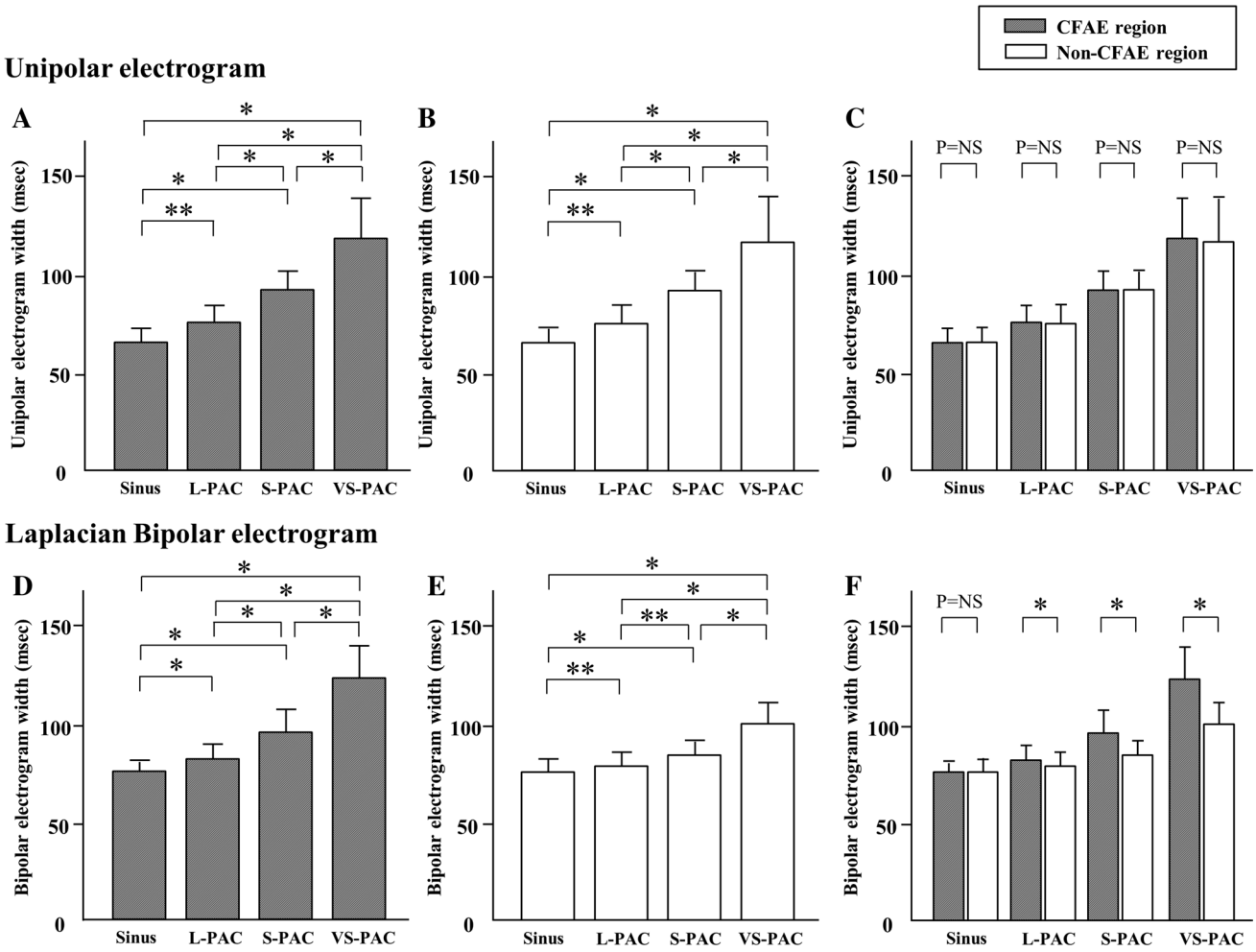

Fig. 2 Unipolar electrogram width during sinus rhythm, L-, S- and VS-PAC in the CFAE region (**a**) and in the non-CFAE region (**b**) are shown. **c** Differences in unipolar electrogram width during sinus rhythm, L-PAC, S-PAC and VS-PAC between the CFAE and the non-CFAE regions. Laplacian bipolar electrogram width during sinus rhythm, L-, S- and VS-PAC in the CFAE region (**d**) and in the non-CFAE region (**e**) are shown. **f** Differences in Laplacian bipolar electrogram width during sinus rhythm, L-PAC, S-PAC and VS-PAC between the CFAE and the non-CFAE regions $*p < 0.001$, $**p < 0.01$

decreased following shortening of the coupling interval of PAC in both the CFAE and non-CFAE sites. The amplitudes in CFAE site during sinus rhythm, L-, S- and VS-PAC (2.52, 1.12, 0.98 and 0.58 mV) were higher than those in the non-CFAE site (1.11, 0.85, 0.77 and 0.47 mV). Prolongation of the electrogram width was noted following shortening of the coupling interval of PAC in both the CFAE and non-CFAE sites. However, the electrogram width in CFAE site during sinus rhythm, L-, S- and VS-PAC (62, 70, 85 and 103 ms) was similar to that in the non-CFAE site (62, 78, 85 and 102 ms).

Comparison of conduction velocity between CFAE and non-CFAE

Shortening of the coupling interval of PAC was associated with a decrease in the conduction velocity in both the CFAE (Fig. 6a) and non-CFAE regions (Fig. 6b). However, the conduction velocity during sinus rhythm, L-, S- and VS-PAC in the CFAE region was significantly slower than that in the non-CFAE region (1.7 ± 0.3 vs. 2.4 ± 0.4, $p < 0.001$; 1.4 ± 0.3 vs. 2.0 ± 0.5, $p < 0.001$; 1.2 ± 0.3 vs. 1.7 ± 0.5, $p < 0.001$; and, 0.9 ± 0.3 vs. 1.4 ± 0.4 m/s, $p < 0.001$, respectively) (Fig. 6c).

Discussion

Main findings

In this study, we showed that the amplitudes of the unipolar and Laplacian bipolar electrograms in the CFAE region were significantly higher than those in the non-CFAE

region, both during sinus rhythm and PACs with various coupling intervals. Furthermore, the increase in the width of the Laplacian bipolar electrogram in CFAE region following shortening of the coupling intervals of PAC was significantly higher than in the non-CFAE region, suggesting marked decrease in local conductivity in the CFAE region.

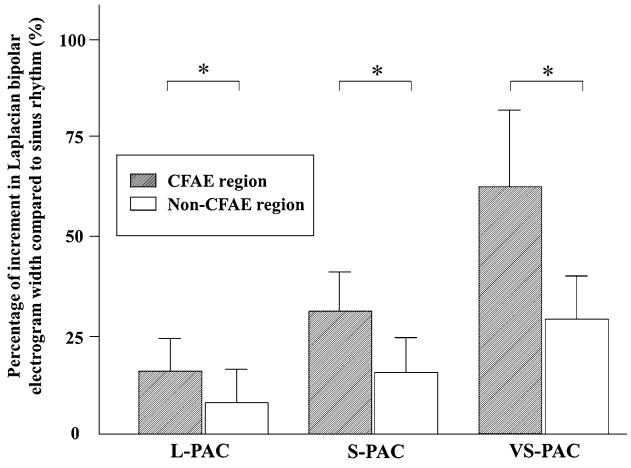

Fig. 3 Comparison of the percentage of increment in Laplacian bipolar electrogram width during L-, S- and VS-PAC relative to the baseline sinus rhythm in the CFAE region (*hatched bars*) and in the non-CFAE regions (*open bars*) *$p < 0.001$

The conduction velocity in the CFAE region was also slower than that in the non-CFAE region. The above findings suggest that CFAE was generated in the high amplitude atrial myocardium with slow and heterogeneous conduction properties, which were markedly associated with premature activation.

Distribution of CFAE with respect to the LA anatomy

CFAE is frequently observed in the inter-atrial septum, PVs and left atrial roof [4]. Furthermore, the CFAE region is stable over time [4, 6, 7], indicating a preferential anatomical site of origin in CFAE. In this study, CFAE was found frequently at the roof, inter-atrial septum and PVs, with high electrogram amplitude. Beinart et al. [8] reported recently that the left atrial roof is significantly thicker than the posterior wall and floor. In comparison, the area of the anterior wall just behind the aorta is usually thin [9]. Ho et al. [10] reported that the superior wall of the LA is thickest. They also found that the sleeve of PV was thickest at the veno-atrial junction, especially in the left superior and right superior PVs [10]. Suenari et al. [11] examined the myocardial thickness using multidetector computed tomography. They found that LA wall was thickest in the left lateral ridge [11]. On the epicardial aspect, the most prominent inter-atrial bundle buttresses and runs in parallel

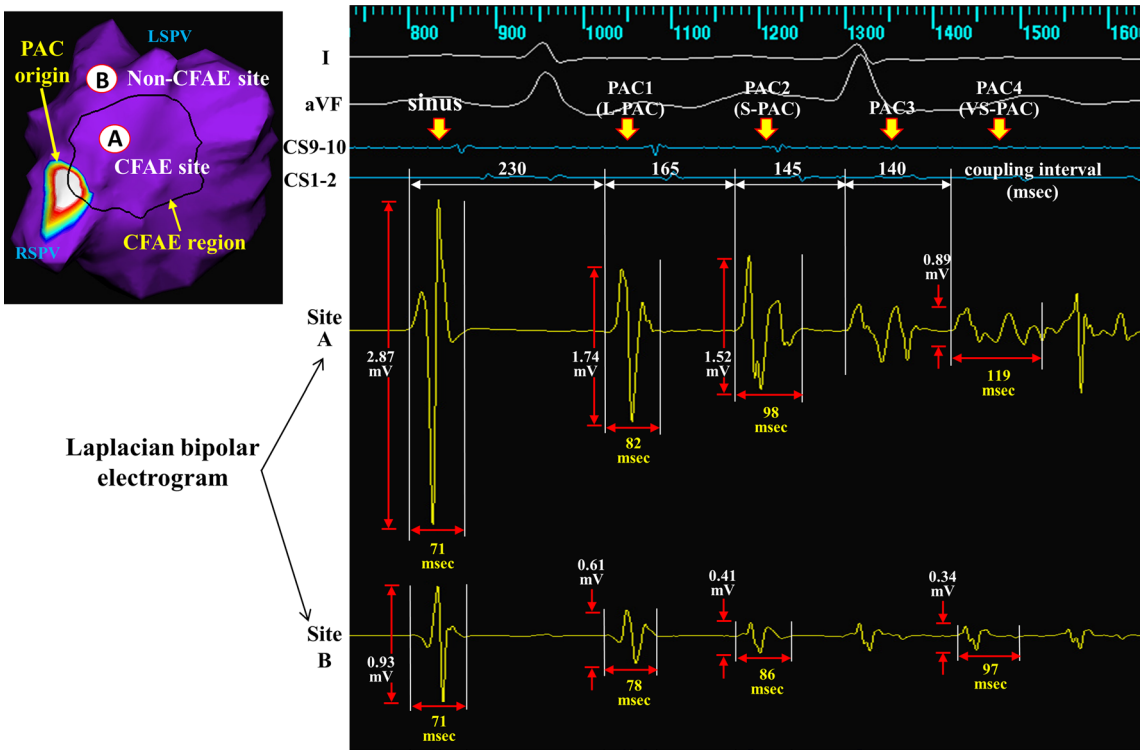

Fig. 4 Laplacian bipolar electrograms during sinus rhythm, L-, S- and VS-PAC in the CFAE site (site *A*) and in non-CFAE site (site *B*) at AF onset are shown. *CS* coronary sinus

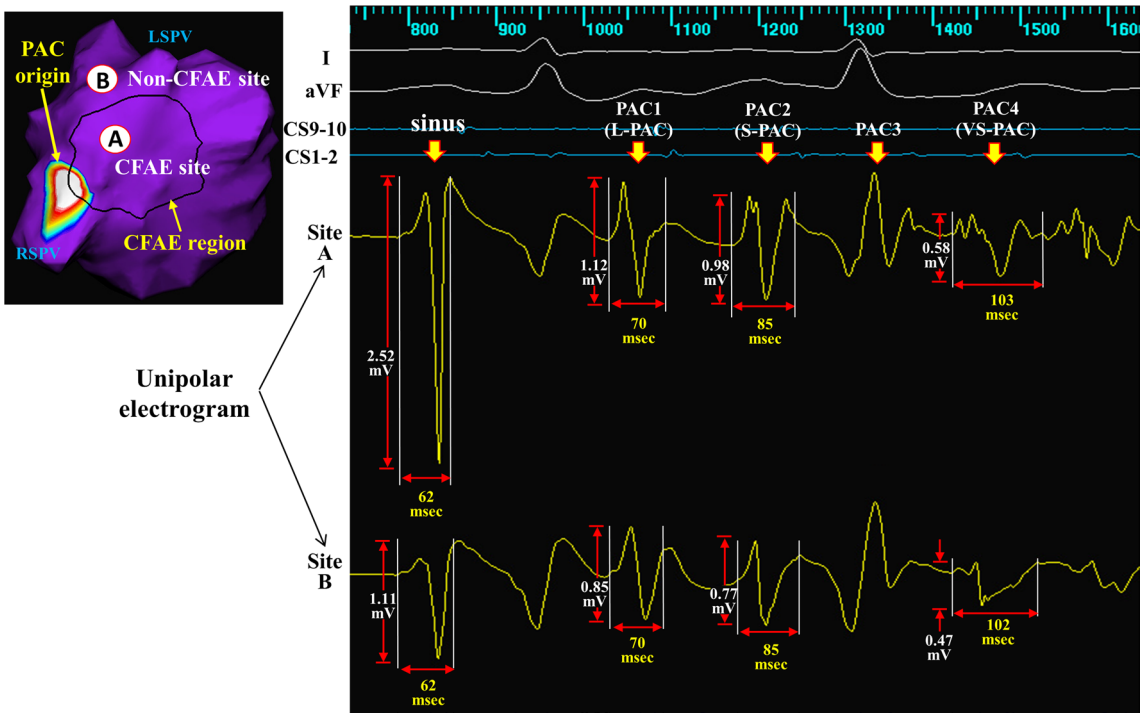

Fig. 5 Unipolar electrogram during sinus rhythm, L-, S- and VS-PAC in the CFAE site (*A*) and in non-CFAE site (*B*) are shown. *CS* coronary sinus

with the circularly arranged left atrial fibers at the superior LA [12]. On the other hand, López-Candales et al. [13] reported that the inter-atrial septum was thicker in patients with AF than in those without AF. Indeed, Platonov et al. [14] reported that inter-atrial bundles are not limited to the anteriorly located Bachmann bundle but are rather present in all parts of the inter-atrial septum. Our findings add support to the above studies that the roof, PVs and the septum are the preferable site of CFAE region with high amplitude atrial electrograms.

Comparison of conductivity in the CFAE and non-CFAE regions

In the present study, a similar prolongation of the width of the unipolar electrogram was noted in the CFAE and non-CFAE regions following shortening of the coupling interval of PAC. This similarity was due to the fact that the unipolar electrogram contains substantial far-field signals generated by depolarization of tissue remote from the recording electrode [15]. In contrast, the width of the Laplacian bipolar electrogram was significantly wider in the CFAE region than in the non-CFAE region during L-, S- and VS-PAC. Since the bipolar electrograms are unaffected by the far-field signals, it leaves the local signals [15]. Therefore, the augmented increase in the width of the Laplacian bipolar electrogram in the CFAE region suggests a decrease in local conductivity in the CFAE area. Spach et al. reported that depressed conduction velocity reduces the amplitude and broaden the duration of electrogram [16], being consistent of the present study. Indeed, the conduction velocities during sinus rhythm, L-, S- and VS-PAC in the CFAE region were all slower than in the non-CFAE region. As shown in the previous study, there is a close relationship between atrial conduction delay and atrial remodeling [17]. A slower conduction in the CFAE region has also been reported previously [5]. These findings indicate the presence of low conductivity in the CFAE region, despite the high amplitude electrograms.

Genesis of CFAE in the high amplitude area of LA

Heterogeneity and CFAE

Sasaki et al. [18] reported that myocardial wall thickness remained significantly associated with local bipolar and unipolar voltage. This finding indicated that thicker myocardial tissue produces high amplitudes. Ho et al. [12] found that there are at least three or more overlapping muscle layers, each with a different fiber direction, especially in the region of roof and septum. Moreover, Platonov et al. [14] also indicated that the inter-atrial bundle was joined inferiorly at the septal raphe. Furthermore, they found that the fossa ovalis is connected with the right inferior and

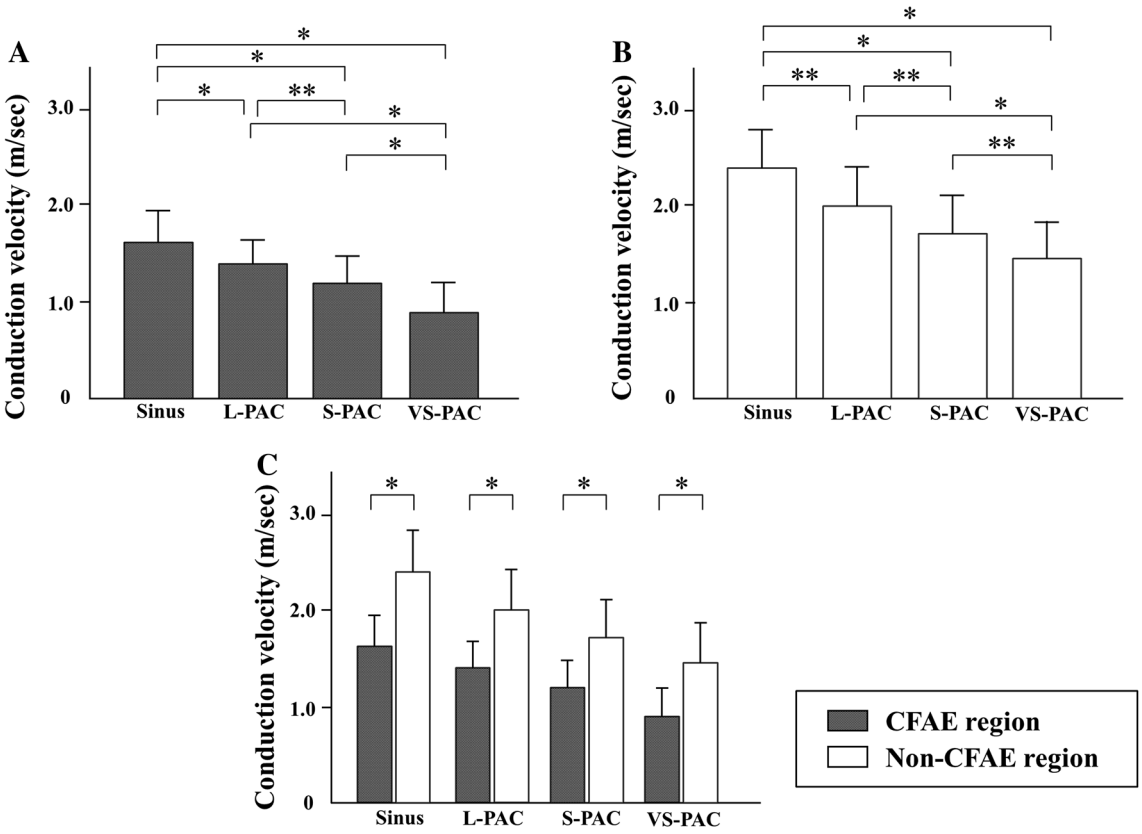

Fig. 6 Conduction velocity during sinus rhythm, L-PAC, S-PAC and VS-PAC in the CFAE region (**a**) and in non-CFAE region (**b**) are shown. **c** Differences in conduction velocity during sinus rhythm, L-, S- and VS-PAC between the CFAE and non-CFAE regions $*p < 0.001$, $**p < 0.01$

superior PVs by a major muscle bundle [14]. Superiorly, it blends with the broadband circumferential fibers that arise from the anterosuperior part of the septal raphe then sweeps leftward into the left lateral wall [10]. Marrouche et al. [19] also showed that there are often three or four overlapping layers in the thicker part of the fossa ovalis. Furthermore, Tagawa et al. [20] reported that the myocardial sleeves in PVs often consisted of two layers. They also found a layer that ran in an oblique direction between these two layers. These findings indicate the presence of heterogeneous myocardial structures in the thicker part of the LA, especially in the roof, septum and PVs. Indeed, Spach et al. [21] reported that atrial conductivity is highly dependent on the specific structural arrangement of cellular connections, suggesting that the thicker part of LA with heterogeneous structure provides the substrate of CFAE.

Fibrosis and CFAE

Spach et al. [22] indicated that interstitial fibrosis may lead to disruption of side-to-side electrical connections, impaired conduction, and the appearance of fractionated electrograms in aging atria. The study of Jacquemet et al. [23] added support to the above by demonstrating the consistent occurrence of CFAEs in regions of fibrosis. Another group also demonstrated enhanced myocardial fibrosis at CFAE sites, compared with non-CFAE sites [24]. Indeed, collagen deposition has been documented in patients with lone AF [25]. Whereas, Wi et al. [26] have shown that LA wall was thicker at CFAE sites than at non-CFAE sites. Thus, they suggested that CFAE may be associated with an intermediate degree of electro anatomical remodeling in the LA, but not with excessively progressed remodeling [26]. Consider together, local fibrosis alone does not contribute to the genesis of CFAE, but increased fibrosis in the thicker atrial wall may be associated with the heterogeneous conduction produced in the CFAE region. Furthermore, pronounced endo-epicardial electrical dissociation, which is related to electrogram fractionation, has been reported in the thickest parts of the atrial wall [27]. Histological analysis also confirmed a major increase in intermyocyte distances due to enhanced extracellular matrix formation. Electrophysiologically, the endo-epicardial electrical dissociation, which was pronounced in the thicker atrium, enhances the coexistence of multiple wavelets, which form the prerequisite for transmural conduction, leading

to increased AF stability [27]. These results indicate that existence of fibrosis in the thicker part of LA with high amplitude electrogram may be associated with generation of CFAE.

Study limitation

Although no patients with multiple PAC origin was presented in this study, several previous studies reported that there were multiple PAC origins which initiate AF. Hioki et al. [28] reported that multiple PACs initiate AF. Lee et al. [29] also reported that 20 % of the patients with PAF had both PV and non-PV ectopic beats. Although we could not evaluate the difference in the local activation properties following the shift in the PAC origin, this needs to be clarified.

Matsuo et al. [30] had shown that both pulmonary vein isolation and linear ablation diminished the CFAE region. Kumagai et al. also reported that most CFAEs that are eliminated by nifekalant after box isolation may be a bystander CFAE, while nifekalant resistant CFAE may be a culprit for AF perpetuation. Therefore, ablation of only CFAEs localized with nifekalant may be sufficient for clinical efficacy [31]. Considering together, these findings suggest the presence of bystander CFAE and active CFAE region. Comparison of the electrophysiological parameters of CFAE region before and after radiofrequency ablation or administration of antiarrhythmic drug may clarify the differences. However, in this study, the data were sampled only before radiofrequency catheter ablation. Therefore, this warrants further investigation.

We used the Laplacian bipolar electrogram in this study. The Laplacian signal calculated as the difference between the signals at the target electrode and the weight sum of eight surrounding electrodes at equidistant. Laplacian electrogram reflects the local transmembrane current [32]. It has also been demonstrated that the amplitude of the Laplacian signals can be correctly displayed under the sufficiently short interelectrode distance [33]. The Laplacian electrogram reveals only the local activation in the same manner as the bipolar electrogram [32]. These suggest that the Laplacian bipolar electrogram sufficiently reflects the real bipolar electrograms although it was not the same.

Conclusions

The CFAE were generated in the high amplitude atrial myocardium with slow and heterogeneous conduction properties which were markedly associated with premature activation. These suggest that anisotropic conduction produced in a high amplitude region may contribute to the genesis of CFAE.

Conflict of interest The authors declare that they have no conflict of interest.

References

1. Hayward RM, Upadhyay GA, Mela T, Ellinor PT, Barrett CD, Heist EK, Verma A, Choudhry NK, Singh JP (2011) Pulmonary vein isolation with complex fractionated atrial electrogram ablation for paroxysmal and nonparoxysmal atrial fibrillation: a meta-analysis. Heart Rhythm 8:994–1000
2. Nademanee K, Lockwood E, Oketani N, Gidney B (2010) Catheter ablation of atrial fibrillation guided by complex fractionated atrial electrogram mapping of atrial fibrillation substrate. J Cardiol 55:1–12
3. Konings KT, Smeets JL, Penn OC, Wellens HJ, Allessie MA (1997) Configuration of unipolar atrial electrograms during electrically induced atrial fibrillation in humans. Circulation 95:1231–1241
4. Nademanee K, McKenzie J, Kosar E, Schwab M, Sunsaneewitayakul B, Vasavakul T, Khunnawat C, Nagarmukos T (2004) A new approach for catheter ablation of atrial fibrillation: mapping of the electrophysiologic substrate. J Am Coll Cardiol 43:2044–2053
5. Yamabe H, Morihisa K, Tanaka Y, Uemura T, Enomoto K, Kawano H, Ogawa H (2009) Mechanisms of the maintenance of atrial fibrillation: role of the complex fractionated atrial electrogram assessed by noncontact mapping. Heart Rhythm 6:1120–1128
6. Yamabe H, Morihisa K, Koyama J, Enomoto K, Kanazawa H, Ogawa H (2011) Analysis of the mechanisms initiating random wave propagation at the onset of atrial fibrillation using noncontact mapping: role of complex fractionated electrogram region. Heart Rhythm 8:1228–1236
7. Scherr D, Dalal D, Cheema A, Nazarian S, Almasry I, Bilchick K, Cheng A, Henrikson CA, Spragg D, Marine JE, Berger RD, Calkins H, Dong J (2009) Long- and short-term temporal stability of complex fractionated atrial electrograms in human left atrium during atrial fibrillation. J Cardiovasc Electrophysiol 20:13–21
8. Beinart R, Abbara S, Blum A, Ferencik M, Heist K, Ruskin J, Mansour M (2011) Left atrial wall thickness variability measured by CT scans in patients undergoing pulmonary vein isolation. J Cardiovasc Electrophysiol 22:1232–1236
9. MacAlpine WA (1975) Heart and coronary arteries: an anatomical atlas for clinical diagnosis, radiological investigation, and surgical treatment. Springer, Berlin, pp 58–59
10. Ho SY, Sanchez-Quintana D, Cabrera JA, Anderson RH (1999) Anatomy of the left atrium: implications for radiofrequency ablation of atrial fibrillation. J Cardiovasc Electrophysiol 10:1525–1533
11. Suenari K, Nakano Y, Hirai Y, Ogi H, Oda N, Makita Y, Ueda S, Kajihara K, Tokuyama T, Motoda C, Fujiwara M, Chayama K, Kihara Y (2013) Left atrial thickness under the catheter ablation lines in patients with paroxysmal atrial fibrillation: insights from 64-slice multidetector computed tomography. Heart Vessels 28:360–368
12. Ho SY, Anderson RH, Sanchez-Quintana D (2002) Atrial structure and fibres: morphologic bases of atrial conduction. Cardiovasc Res 54:325–336
13. López-Candales A, Grewal H, Katz W (2005) The importance of increased interatrial septal thickness in patients with atrial fibrillation: a transesophageal echocardiographic study. Echocardiography 22:408–414

14. Platonov PG, Mitrofanova L, Ivanov V, Ho SY (2008) Substrates for intra-atrial and interatrial conduction in the atrial septum: anatomical study on 84 human hearts. Heart Rhythm 5:1189–1195
15. Issa ZF, Miller JM, Zipes DP (2012) A companion to Braunwald's heart disease, 2nd edn. WB Saunders, Philadelphia, pp 72–73
16. Spach MS, Barr RC, Serwer GA, Kootsey JM, Johnson EA (1972) Extracellular potentials related to intracellular action potentials in the dog Purkinje system. Circ Res 5:505–519
17. Maeno K, Kasai T, Kasagi S, Kawana F, Ishiwata S, Ohno M, Yamaguchi T, Narui K (2013) Relationship between atrial conduction delay and obstructive sleep apnea. Heart Vessels 28:639–645
18. Sasaki T, Miller CF, Hansford R, Yang J, Caffo BS, Zviman MM, Henrikson CA, Marine JE, Spragg D, Cheng A, Tandri H, Sinha S, Kolandaivelu A, Zimmerman SL, Bluemke DA, Tomaselli GF, Berger RD, Calkins H, Halperin HR, Nazarian S (2012) Myocardial structural associations with local electrograms: a study of postinfarct ventricular tachycardia pathophysiology and magnetic resonance-based noninvasive mapping. Circ Arrhythm Electrophysiol 5:1081–1090
19. Marrouche NF, Natale A, Wazni OM, Cheng J, Yang Y, Pollack H, Verma A, Ursell P, Scheinman MM (2004) Left septal atrial flutter: electrophysiology, anatomy, and results of ablation. Circulation 109:2440–2447
20. Tagawa M, Higuchi K, Chinushi M, Washizuka T, Ushiki T, Ishihara N, Aizawa Y (2001) Myocardium extending from the left atrium onto the pulmonary veins: a comparison between subjects with and without atrial fibrillation. Pacing Clin Electrophysiol 24:1459–1463
21. Spach MS, Miller WT 3rd, Dolber PC, Kootsey JM, Sommer JR, Mosher CE Jr (1982) The functional role of structural complexities in the propagation of depolarization in the atrium of the dog. Cardiac conduction disturbances due to discontinuities of effective axial resistivity. Circ Res 50:175–191
22. Spach MS, Dolber PC (1986) Relating extracellular potentials and their derivatives to anisotropic propagation at a microscopic level in human cardiac muscle. Evidence for electrical uncoupling of side-to-side fiber connections with increasing age. Circ Res 58:356–371
23. Jacquemet V, Henriquez CS (2009) Genesis of complex fractionated atrial electrograms in zones of slow conduction: a computer model of microfibrosis. Heart Rhythm 6:803–810
24. Liu X, Shi HF, Tan HW, Wang XH, Zhou L, Gu JN (2009) Decreased connexin 43 and increased fibrosis in atrial regions susceptible to complex fractionated atrial electrograms. Cardiology 114:22–29
25. Frustaci A, Chimenti C, Bellocci F, Morgante E, Russo MA, Maseri A (1997) Histological substrate of atrial biopsies in patients with lone atrial fibrillation. Circulation 96:1180–1184
26. Wi J, Lee HJ, Uhm JS, Kim JY, Pak HN, Lee M, Kim YJ, Joung B (2014) Complex fractionated atrial electrograms related to left atrial wall thickness. J Cardiovasc Electrophysiol 25:1141–1149
27. Eckstein J, Maesen B, Linz D, Zeemering S, van Hunnik A, Verheule S, Allessie M, Schotten U (2011) Time course and mechanisms of endo-epicardial electrical dissociation during atrial fibrillation in the goat. Cardiovasc Res 89:816–824
28. Hioki M, Matsuo S, Yamane T, Tokutake K, Ito K, Narui R, Tanigawa S, Yamashita S, Tokuda M, Inada K, Date T, Yoshimura M (2012) Adenosine-induced atrial tachycardia and multiple foci initiating atrial fibrillation eliminated by catheter ablation using a non-contact mapping system. Heart Vessels 27:221–226
29. Lee SH, Tai CT, Hsieh MH, Tsao HM, Lin YJ, Chang SL, Huang JL, Lee KT, Chen YJ, Cheng JJ, Chen SA (2005) Predictors of non-pulmonary vein ectopic beats initiating paroxysmal atrial fibrillation: implication for catheter ablation. J Am Coll Cardiol 46:1054–1059
30. Matsuo S, Yamane T, Date T, Tokutake K, Hioki M, Narui R, Ito K, Tanigawa S, Yamashita S, Tokuda M, Inada K, Arase S, Yagi H, Sugimoto K, Yoshimura M (2012) Substrate modification by pulmonary vein isolation and left atrial linear ablation in patients with persistent atrial fibrillation: its impact on complex-fractionated atrial electrograms. J Cardiovasc Electrophysiol 23:962–970
31. Kumagai K, Toyama H (2013) Usefulness of ablation of complex fractionated atrial electrograms using nifekalant in persistent atrial fibrillation. J Cardiol 61:44–48
32. Shenasa M, Hindricks G, Borggrefe M, Breithandt G, Josephson ME (2012) Cardiac mapping, 4th edn. Wiley-Blackwell, Oxford, pp 1–11
33. Coronel R, Wilms-Schopman FJ, de Groot JR, Janse MJ, van Capelle FJ, de Bakker JM (2000) Laplacian electrograms and the interpretation of complex ventricular activation patterns during ventricular fibrillation. J Cardiovasc Electrophysiol 11:1119–1128